Stark broadening of C IV and N V lines in the vacuum-uv spectral range

F. Böttcher, J. Musielok,* and H.-J. Kunze
Institut für Experimentalphysik, Ruhr-Universität, 4630 Bochum, Federal Republic of Germany
(Received 3 March 1987)

Spectral line shapes of $3p$-$4d$, $3d$-$4f$, $4d$-$5f$, and $4f$-$5g$ transitions in the lithiumlike ions C IV and N V have been measured in a gas-liner pinch discharge at a density of 7.7×10^{23} m^{-3}. The full widths at half maximum are larger than theoretical values obtained by the impact approximation by factors between 3 and 4 and smaller than theoretical full widths at half maximum calculated in the quasistatic, linear Stark effect approximation by factors between 1.2 and 3.

I. INTRODUCTION

Lithiumlike ions have been discussed as possible candidates for extending the scheme of plasma recombination lasers into the vacuum-uv (vuv) spectral region. $3p$-$4d$ and $3d$-$4f$ transitions appeared to be especially promising.[1] The expected gain of a laser transition depends, however, on the spectral width of the transition, and the knowledge of the actual broadening in high-density plasmas still is rather poor. (See, for example, Ref. 2.) In the following we report measurements of such transitions in C IV and N V which supplement and extend previous investigations carried out on the same plasma device.[3]

II. EXPERIMENT

The gas-liner pinch is extensively described in previous publications.[4–6] It is a modified z pinch and was developed to allow measurements of line profiles at high densities and temperatures without certain difficulties which arise usually with normal z-pinch discharges. The crux is a special gas inlet system, which injects two independent gas streams into the vacuum of the discharge chamber by means of two fast valves. The driver gas streams as a shell concentrically to the axis with a radius of 8 cm; it absorbs the energy from the outer circuit and is accelerated by the magnetic piston towards the center. The test gas streams along the axis of the discharge chamber. As long as its density is low compared to that of the driver gas, the plasma parameters are essentially determined by the latter, and the test gas is confined to the central homogeneous plasma region with rather constant electron density and temperature: No Abel inversion is necessary for the analysis of the emission from test-gas ions.[3] Furthermore, different test gases can easily be used without changing the plasma parameters. We have used hydrogen as the driver gas and methane, nitrogen, and helium as test gases to observe spectral lines of C IV, N V and He II respectively, the latter one merely for diagnostics purposes. Since spectral lines in the vuv spectral range are usually strong, a small amount of test gas of about 1% of the driver-gas density was sufficient to obtain a good line to continuum intensity ratio. For the present measurements, the main parameters of the gas-liner pinch were 5 cm distance between the electrodes, 8 cm radius of the discharge chamber, 1.2 kJ stored electrical energy, and a 3-μs period of the discharge. The plasma column had a radius of 8 mm at maximum compression and was observed side on. It existed for about 400 ns with a full width at half maximum of about 200 ns. The plasma parameters are discussed in Sec. III.

The experimental setup is shown in Fig. 1. The continuum emission at 537.6 and 544.2 nm is used to monitor the plasma for the test gases nitrogen and methane, respectively: It is recorded via a $\frac{1}{4}$-m monochromator equipped with a photomultiplier at the exit slit.

This monitor allows us to judge the reproducibility of the discharge and to obtain the time difference between the maximum compression of the plasma and the time

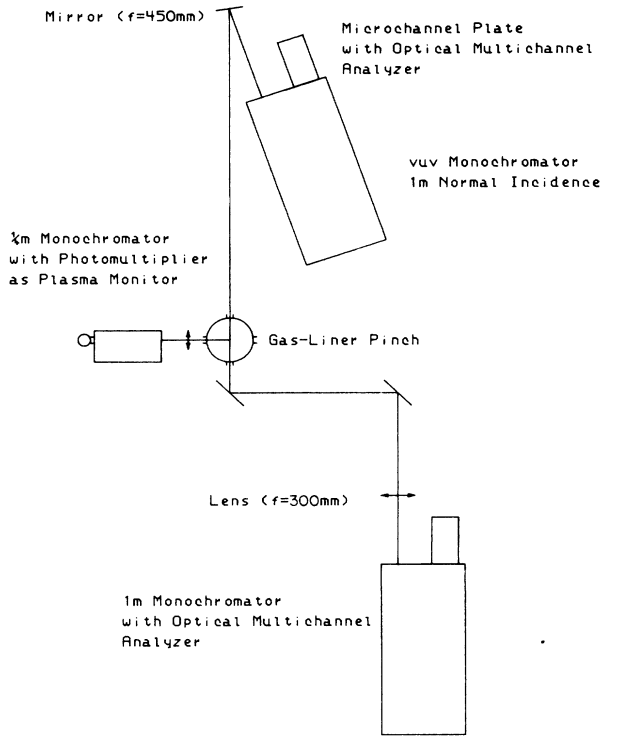

FIG. 1. Experimental setup.

when the multichannel analyzers described below are gated.

The line profiles in the visible and ultraviolet spectral region were recorded by an optical multichannel analyzer system (EG&G model OMA II). The monochromator used (1-m Czerny-Turner type, Spex model 1704 with a 1200-lines/mm grating) had a reciprocal dispersion of 0.83 nm/mm corresponding to 0.02 nm/channel of the OMA system. The apparatus profile was a Voigt profile with approximately five channels full width at half maximum intensity (FWHM) for an entrance slit of 25 μm width. The detector head was gated with a nearly rectangular voltage pulse of -200 V and 20 ns duration to obtain an appropriate time resolution.

For the observation in the vacuum-uv region, a 1-m normal incidence spectrometer (McPherson model 225 with a concave grating of of 1200 lines/mm) was available. The reciprocal dispersion was 0.83 nm/mm with an entrance slit of 25 μm. Because of the special properties of the gas-liner pinch, no differential pumping equipment was necessary. A concave mirror (MgF_2 coated) was used to image the plasma column onto the entrance slit. In order to eliminate the uncertainties which result from scanning the line profiles in the vacuum-uv region from discharge to discharge, we tested and employed a detection system which allowed recording of the total profile during preselectable time intervals of the discharge. It consisted, in principle, of a microchannel plate (MCP)[7] followed by the optical multichannel analyzer system discussed above for the visible spectral region. A schematic of the arrangement is shown in Fig. 2. A chevron pair of MCP's with 12-μm channel diameter (Galileo model 3025 with CsI coating on the input side and a P20 phosphor at the exit) was placed in the exit plane of the vuv monochromator. The maximum voltage allowed for each plate was 1 kV. The phosphor screen was imaged onto the head of the OMA-II system. For good time resolution, it was necessary to gate the detection system. We gated the first plate with a nearly rectangular voltage pulse of -700 V and a duration of 30 ns. The voltage across the second plate was constant and was chosen between -500 V and -800 V depending on the vuv line intensity in order to avoid saturation of the OMA- detector head. If the first plate was not gated, no light was observed. The linearity of the response versus the intensity of the plasma radiation was tested for constant MCP voltages by putting different numbers of micromeshes into the light path. The wavelength calibration was performed with an argon miniarc[8] (both plates of the MCP at constant voltage) and with various resonance lines of the test gas in the whole accessible wavelength range. The reciprocal dispersion turned out to be 0.0209 nm/channel in the first order. The upper wavelength limit of about 200 nm was essentially due to the rapid decrease of the MCP detection efficiency; the lower wavelength limit of approximately 30 nm was mainly determined by the poor transmission properties of the normal incidence monochromator because the efficiency of the MCP increases with decreasing wavelength. The efficiency of the MCP and the reflectivity of the mirror are functions of wavelength with opposite slopes, and it is not easy to compare line intensities in different wavelength regions. However, by observing the continuum from the miniarc and plasma discharges we found that the overall efficiency of the detection system is practically constant over the wavelength range for which a spectrum, i.e., usually a line profile, is recorded. To determine the apparatus profile, we observed the transition N I $^2P^0$-^2D at 141.2 nm of the argon miniarc operated at 15 A. The Doppler and Stark broadening of this line are negligible compared to the

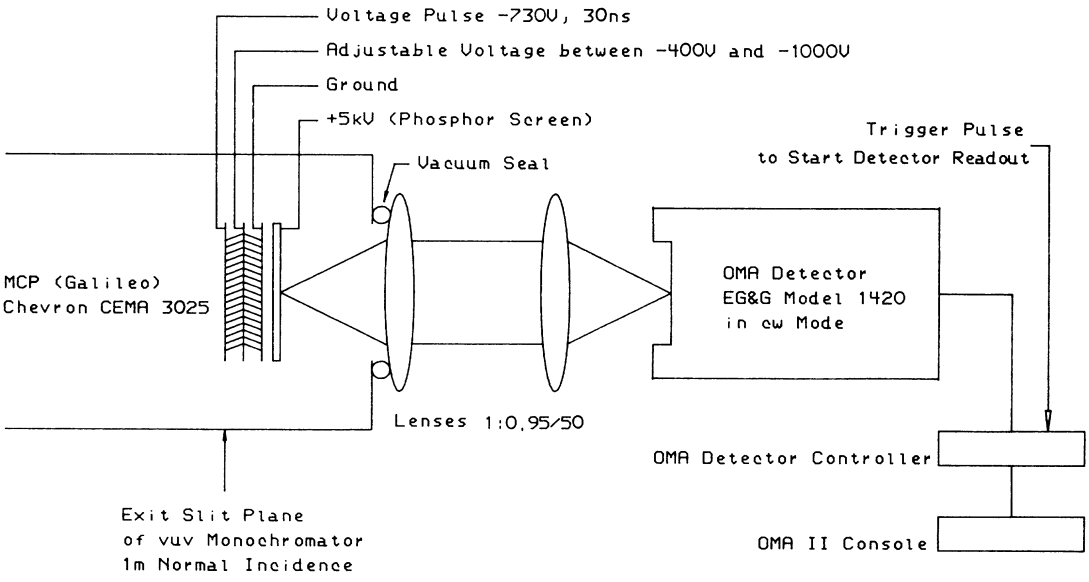

FIG. 2. Schematic drawing of the vacuum-uv detection system.

resolution of the detection system. The apparatus profile was a Voigt profile with 0.01 nm Gaussian FWHM and 0.17 nm Lorentzian FWHM, both in the first order. Since we were not restricted to the first order, this resolution was sufficient for all measured lines. This apparatus profile was confirmed for the whole wavelength range by many (resonance) lines of the test gas [see for example Fig. 4(b) below]; of course, here one has to take into account the Doppler broadening.

III. MEASUREMENTS

The electron temperature of the plasma was determined from the line intensity ratio of two line pairs in the visible and in the vuv region, based on a calculation of line intensity ratios in the ultraviolet by Griem.[9] This calculation can be modified to use the line intensity ratio I(C IV 465.8 nm)/I(C III 464.7 nm) in the visible or the line intensity ratio I (C IV 116.9 nm)/I (C III 117.6 nm) in the vuv region [(see Fig. 5 (a) and (b) below].

The comparison between the temperatures derived from the two line pairs shows good agreement. The absolute accuracy of the temperature is about 30% and is essentially determined by the uncertainties in the theoretical intensity ratio. A second independent temperature determination had been performed previously for almost the same conditions.[10] There the temperature was obtained from the blackbody limited intensity of the C IV resonance transition which was optically thick.

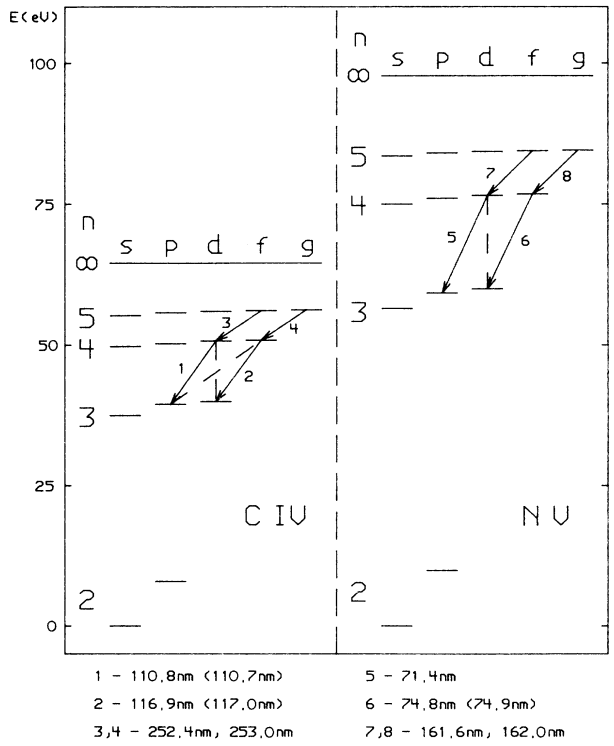

FIG. 3. Grotrian diagram of the Li-like C IV and N V ions. Solid arrows indicate measured dipole allowed transitions, dashed lines indicate the observed forbidden lines.

The electron density was derived from the measured FWHM of the He II $P\alpha$ line at 468.6 nm using the empirical relationship proposed by Pittman and Fleurier.[11] Ackermann *et al.*[3] recently confirmed the validity of this relationship in the present device for nearly the same plasma conditions. The accuracy of this formula itself is estimated to about 10%, and the uncertainty of the electron density determination caused by the irreproducibility of the discharge does not exceed 15%.

The observed line profiles in the vuv are all measured at maximum compression of the plasma when the electron density was 7.7×10^{23} m^{-3} and the electron (and ion) temperature was 10.7 eV. To show certain effects in the line profile of two C IV lines, we have measured these lines also at the time of 120 ns after maximum compression: The electron density was 4.7×10^{23} m^{-3} and the temperature 9.8 eV. The Grotrian diagram for all observed lines is shown in Fig. 3.

The transitions C IV 3-4 and N V 4-5 are measured in second order, the transitions N V 3-4 in fourth order, and the transition C IV 4-5 in the ultraviolet region in the first order. To estimate the influence of any finite optical depths on the line profiles, we have increased the amount of test-gas methane up to a factor of 10 until the C IV 2*s*-

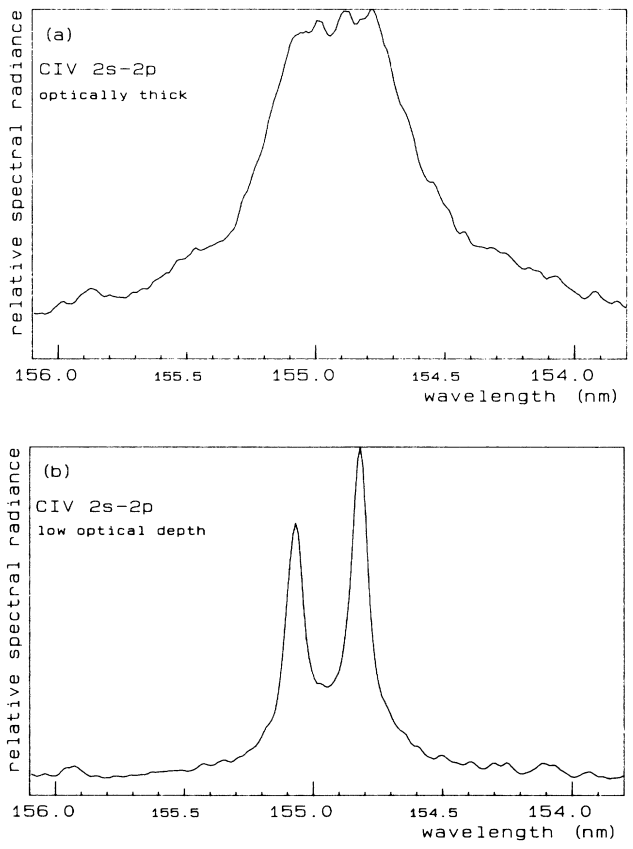

FIG. 4. C IV resonance line 2*s*-2*p* with different test gas amounts (test gas methane) at maximum compression. For achieving the optically thick line, we used 10 times more test gas than in the case with low optical thickness.

$2p$ transition was optically thick (see Fig. 4). If one takes into account the differences in transition probabilities between the C IV resonance line and the observed lines and the different excitation energies of the levels involved (see Fig. 3), the optical depths of all measured lines are far below one. The effect of radiative transport on the line profiles is therefore negligible.

All measured line profiles are shown in Figs. 5 to 7. It has to be mentioned that the spectra are averages over about eight single spectra and that the y axes are linear but different for each profile shown.

Since for the vuv spectra no background subtraction was performed, one can see that the intensity ratio of the radiation in the line core to the continuum is larger than 4 in all cases. For each line studied, we measured the background radiation by operating the gas-liner pinch without test gas. These measurements revealed that the lines were not perturbed by impurity lines and only continuum emission arising from various orders was responsible for the measured background signals. In some cases we have used a LiF window to eliminate perturbing lines in higher orders.

IV. RESULTS AND DISCUSSION

The energy levels of C IV and N V ions show a typical doublet structure. All transitions between excited levels therefore consist of three line components, two transitions with $\Delta J=1$ and one with $\Delta J=0$. As an example, Fig. 8

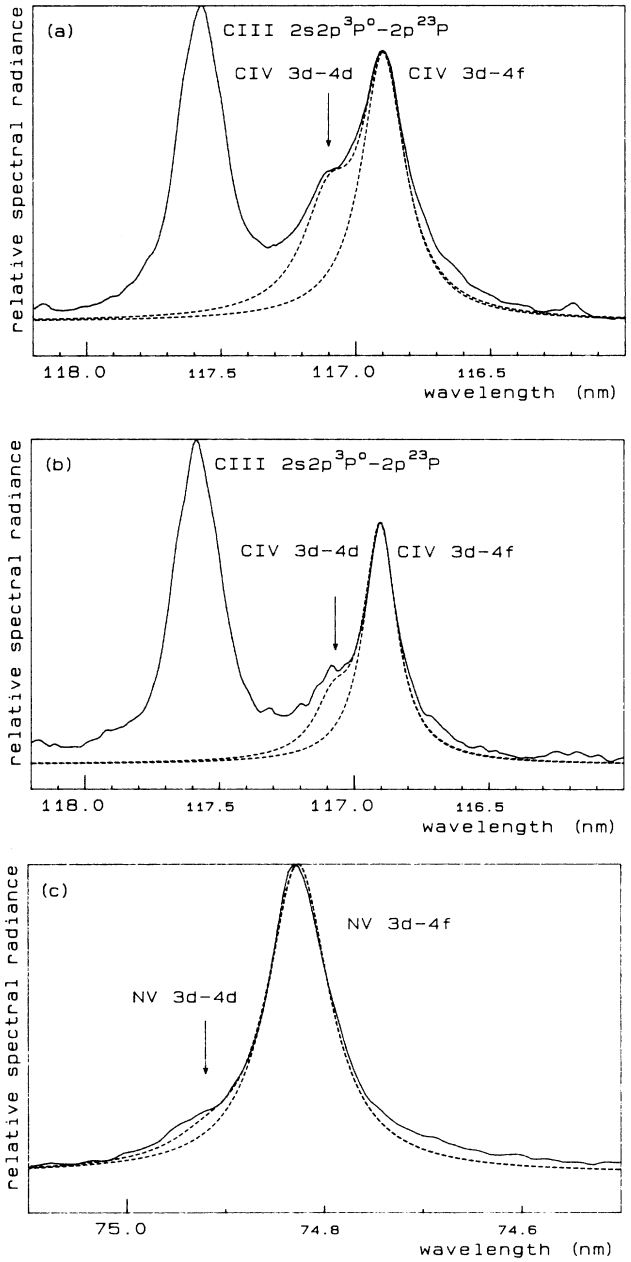

FIG. 5. (a) and (c) $N_e = 7.7\times10^{23}$ m^{-3}, $kT_e=10.7$ eV; (b) $N_e=4.7\times10^{23}$ m^{-3}, $kT_e=9.8$ eV. Comparison of measured (solid) and computed (dashed) line profiles of the transition $3d$-$4f$. Two computed line profiles are shown for each spectrum. One profile consists of the three fine-structure components; the contribution of the forbidden component $3d$-$4d$ is taken into account in the other profile. The arrows indicate the respective wavelengths of the forbidden component.

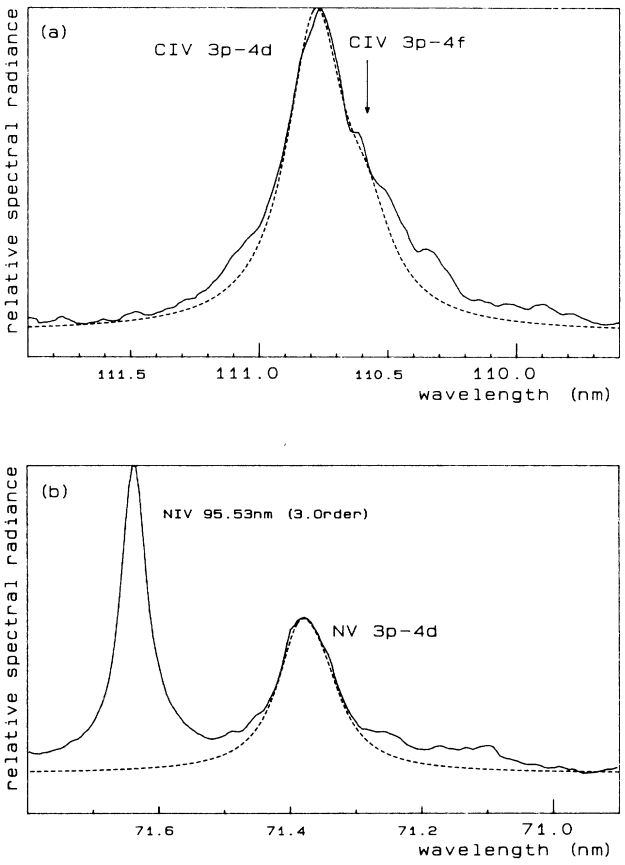

FIG. 6. $N_e=7.7\times10^{23}$ m^{-3}, $kT_e=10.7$ eV. Comparison of measured (solid) and computed (dashed) line profiles of the transition $3p$-$4d$. (a) For the computed profile the forbidden component $3p$-$4f$ is taken into account. (b) No clear evidence for the forbidden component was found.

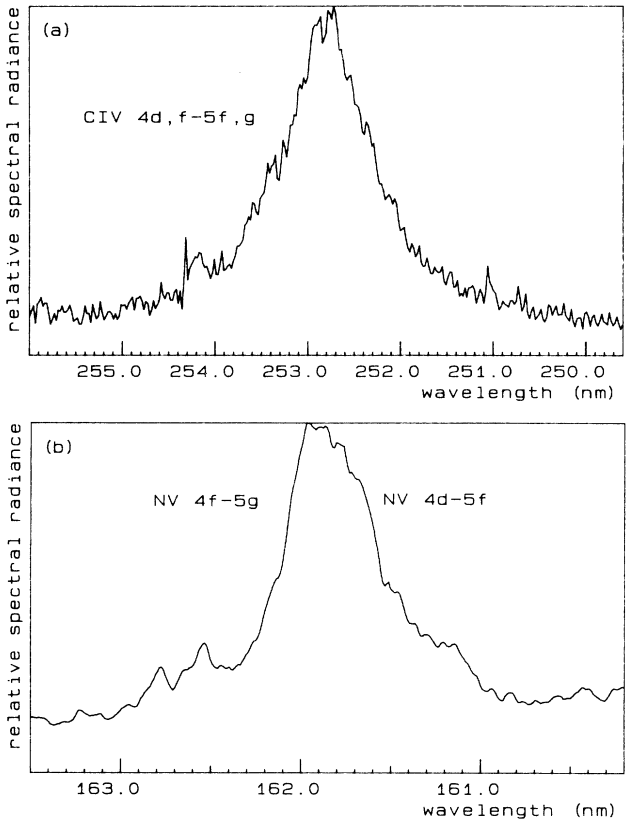

FIG. 7. $N_e = 7.7 \times 10^{23}$ m^{-3}, $kT_e = 10.7$ eV. Experimental line profiles of the transition $4d,f$-$5f,g$. Because of strong level mixing the line shape is similar to hydrogenlike transitions. The C IV line (a) was measured with the monochromator for the visible and uv spectral range.

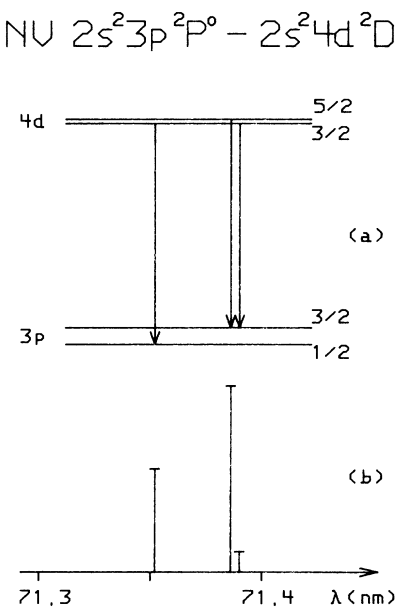

FIG 8. (a) Fine-structure splitting and (b) corresponding line components of the N V $3p$-$4d$ transition. The intensities of the line components are calculated assuming LS coupling.

shows the fine-structure splitting and the corresponding line components of the N V $3p$-$4d$ transition. The intensities were calculated assuming LS coupling.

The line profiles emitted from the plasma are governed by Doppler and Stark broadening. The Doppler broadening for each line was calculated from the plasma temperature. Other broadening mechanisms can be neglected for our plasma conditions. The profiles shown are additionally influenced by the apparatus profile.

For our line profile study two different theoretical approaches are available: the impact and the quasistatic approximation[12] although, for a given transition, the two approximations are valid only for a certain range of plasma parameters. For our plasma conditions we are in a range where both approximations are not strictly valid.

According to the semiempirical impact approximation given by Griem,[12] the Stark broadening of each line reflects the broadening of the upper and lower energy levels. The broadening of the level (n,l) is governed mainly by electron collisions with the levels $(n,l-1)$ and $(n,l+1)$. The contributions from $\Delta n \neq 0$ inelastic and strong collisions are usually relatively small. For all transitions with $\Delta n \neq 0$ the contribution of the upper level to the broadening of the spectral line is dominant (see, for example, Ref. 3). Using formula 526 of Ref. 12 for the upper and lower levels, which includes all collision processes mentioned, we have calculated the width of the Lorentz profile due to Stark broadening. The FWHM for all lines studied are listed in Table I ("$\Delta\lambda_{\mathrm{FWHM}}$, Theory, Collisional"). In the quasistatic and linear Stark effect approximation the fine structure is meaningless and l degeneracy is assumed. Formula 16 of Ref. 12 gives an estimation of the linewidth in this approximation. The derived FWHM's are listed in Table I under the heading "$\Delta\lambda_{\mathrm{FWHM}}$, Theory, Static."

Corresponding to the two different theoretical approximations, two different methods to determine the FWHM due to Stark broadening from the measured spectra are necessary.

The FWHM of the total measured line corrected for Doppler and apparatus profile is included in Table I under "$\Delta\lambda_{\mathrm{FWHM}}$, Experimental Stark Width, Line (Static)" and corresponds to the quasistatic approximation. To find the FWHM appropriate for the impact approximation, we have fitted a superposition of three Voigt profiles to the measured line profile. The wavelength and relative intensities of the three fine-structure components were used for the Voigt profiles. Each of the Voigt profiles consists of the appropriate Doppler and apparatus profile and a Lorentz profile, which reflects the Stark broadening. The FWHM of this Lorentz profile enters Table I under the heading "$\Delta\lambda_{\mathrm{FWHM}}$, Experimental Stark Width, Fine-Structure Component." This fitting process seems to be meaningless for the 4-5 transitions, because the lines cannot be separated in the case of C IV and because no well-fitting profile was found in the case of N V.

The comparison between experimental and theoretical FWHM's shows a reasonable agreement in the case of the quasistatic approximation, with theoretical values systematically exceeding the experimental ones. For a given transition the agreement is better for higher electron den-

TABLE I. Comparison between measured and calculated Stark width.

Transition	Spectrum	Wavelength (nm)	N_e (10^{23} m^{-3})	$\Delta\lambda_{FWHM}$ (nm) Theory (Griem, 1974) Collisional	(Static)	Experimental Stark Width Fine-Structure Component	Line (Static)	Apparatus and Doppler Profile	$\Delta\lambda_{FWHM,expt.}/\Delta\lambda_{FWHM,theory}$ Collisional	Static
$3p$-$4d$	C IV	110.8	7.7	0.044	0.27	0.18[a]	0.23[a]	0.088	4.1	0.85
			4.7	0.027	0.19	0.10[a]	0.12[a]		3.7	0.63
$3p$-$4d$	N V	71.4	7.7	0.011	0.090	0.042[b]	0.065[b]	0.044	3.8	0.72
$3d$-$4f$	C IV	116.9	7.7	0.027	0.30	0.12[c]	0.15[c]	0.088	4.4	0.50
			4.7	0.018	0.22	0.060[c]	0.070[c]		3.3	0.32
$3d$-$4f$	N V	74.8	7.7	0.0071	0.10	0.030[c]	0.033[c]	0.044	4.2	0.33
$4d$-$5f$	C IV	252.4	7.7	0.64	1.8		1.0[b]	0.14		0.56
$4f$-$5g$		253.0		0.35						
$4d$-$5f$	N V	161.6	7.7	0.17	0.58		0.55[c]	0.088		0.95
$4f$-$5g$		162.0		0.086						

[a]Accuracy of experimental data: 25%.
[b]Accuracy of experimental data: 15%.
[c]Accuracy of experimental data: 20%.

sities; for given density and transition the agreement is better for C IV (lower Z emitter). The good agreement in the case of the N V 4-5 transition is accidental: The wavelength difference between the two lines $4d$-$5f$ and $4f$-$5g$ is approximately equal to the theoretical FWHM. Therefore, the full-width at half maximum is not a good measure for the broadening of the line [see Fig. 7(b)].

The discrepancy between experimental and theoretical results for the impact approximation is rather large. The experimental FWHM's exceed the theoretical ones by factors of 3 to 4. Similar discrepancies were found in Ref. 3 for C IV. For our plasma conditions the plasma frequency ω_{pl} is larger than the frequency separation between the levels $4d$ and $4f$, and $5f$ and $5g$, respectively. Therefore, the ω_{pl} value was applied as the cutoff parameter in the calculations of the effective Gaunt factors. If the influence of the plasma frequency is neglected, the calculated FWHM's are slightly larger (but not by more than 25%). In Ref. 3 a comparison of the theoretical FWHM from Griem[12] and Dimitrijević and Konjević[13] had been carried out. Since the later ones are even lower than the FWHM's of Griem, they are not included in Table I.

For the transitions $3d$-$4f$ and $3p$-$4d$ the respective forbidden transitions 3d-4d and 3p-4f influence the line shapes, as can be seen in Figs. 5 and 6. These forbidden transitions had to be taken into account in the fitting process for the impact approximation. In Fig. 5 both theoretical profiles with and without forbidden lines are shown. The fitting parameters were the intensity and wavelength of the forbidden line, whereas the FWHM ratio of allowed and forbidden lines was taken from the impact approximation. The resulting wavelength from the fitting procedure of the forbidden lines are 117.10 nm [Fig. 5(a)] and 117.07 nm [Fig. 5(b)]. As expected from theoretical considerations, the intensity and the shift of the forbidden line decrease with decreasing electron density.

For a given $\Delta n \neq 0$ transition the lower electron density limit to apply the quasistatic approximation[12] is (among other dependencies) proportional to Z^3 ($Z=4$ for C IV, $Z=5$ for N V). Therefore the electron density of 7.7×10^{23} m^{-3} is sufficient to "produce" a rather strong forbidden line in the C IV spectrum in comparison to the corresponding line in N V [see Fig. 5(c)].

V. CONCLUSIONS

Our results show that for our plasma conditions the ion broadening of the level $n=5(l>1)$ has to be treated in the quasistatic approximation and that the level mixing for $n=4$ is already noticeable. For $n=3$ the levels with different l are well separated and can, therefore, be treated in the electron impact approximation, broadening by ions being in the quadratic Stark effect regime and therefore small.

For a given transition and electron density of the plasma the impact theory predicts FWHM (in wavelength units) which are 4 times larger for the C IV spectral lines than for the corresponding lines of N V. The quasistatic theory yields FWHM's 3 times larger for C IV than for N V. Our measurements support this tendency, however, the absolute values of the FWHM disagree by factors of 3 to 4 with the values of the electron impact approximation (the measured values being larger) and by a factor of 1.2 to 3 in the case of the quasistatic, linear Stark effect approximation (the measured values being smaller). For the plasma parameter range of our gas-liner pinch and with the present detection system, Stark broadening measurements for a given transition can be performed only for two subsequent ions in the isoelectronic sequence with reasonable accuracy. To extend the study to other ions of the sequence, plasmas with higher densities and temperature and/or spectrometers with higher resolution are necessary.

ACKNOWLEDGMENT

This work was supported by the Sonderforschungsbereich 162 (Plasmaphysik Bochum/Jülich).

*Permanent address: Institute of Physics, Pedagogical University, 45-052 Opole, Poland.

[1]E. Ya. Kononov and K. N. Koshelev, Kvant. Elektron. (Moscow) **1**, 2411 (1974) [Sov. J. Quantum Electron., **4**, 1340 (1975)].

[2]N. Konjević, M. S. Dimitrijević, and W. L. Wiese, J. Phys. Chem. Ref. Data **13**, 649 (1984).

[3]U. Ackermann, K. H. Finken, and J. Musielok, Phys. Rev. A **31**, 2597 (1985).

[4]K. H. Finken and U. Ackermann, Phys. Lett. **85A**, 279 (1981).

[5]K. H. Finken and U. Ackermann, J. Phys. D **15**, 615 (1982).

[6]K. H. Finken and U. Ackermann, J. Phys. D **16**, 773 (1983).

[7]J. L. Wiza, Nucl. Instrum. Methods **162**, 587 (1979).

[8]J. M. Bridges and W. R. Ott, Appl. Opt. **16**, 367 (1977).

[9]H. R. Griem, *Plasma Spectroscopy* (McGraw-Hill, New York, 1964).

[10]F. Böttcher, U. Ackermann, and H.-J. Kunze, Appl. Opt. **25**, 3307 (1986).

[11]T. L. Pittmann and C Fleurier in *Spectral Line Shapes*, edited by K. Burnett (deGruyter, New York, 1983), Vol. II.

[12]H. R. Griem, *Spectral Line Broadening by Plasmas* (Academic, New York, 1974).

[13]M. S. Dimitrijević and N. Konjević, J. Quant. Spectrosc. Radiat. Transfer **24**, 451 (1980).